



Functional Catastrophe Analysis of Progressive Failures for Deep Tunnel Roof Considering Variable Dilatancy Angle and Detaching Velocity

Kaihang Han^{1,2} · Jiann-Wen Woody Ju² · Heng Kong³ · Mengshu Wang⁴

Received: 3 June 2018 / Accepted: 5 April 2019 / Published online: 29 April 2019
© Springer-Verlag GmbH Austria, part of Springer Nature 2019

Abstract

The phenomena of progressive failures are very common and important in geotechnical engineering. In this paper, a reliable prediction model is proposed to interpret the progressive failure phenomenon of roof collapse in deep tunnels using the functional catastrophe theory. The progressive collapse mechanisms and collapsing block shapes of deep circular tunnels under conditions of plane strain are investigated. The analytical solutions for the shape curves of the collapsing blocks of circular tunnels are derived based on the nonlinear power-law failure criterion considering variable dilatancy angle and detaching velocity. Moreover, criteria with variable dilatancy angle on progressive failure occurrence for deep tunnels are obtained. Then, the analytical predictions obtained in this paper are compared with experimental testing results, which indicate that the impacts of variable detaching velocity on the shape curves of the several continuous collapsing blocks should be considered to obtain more consistent prediction results with the corresponding experimental testing results.

Keywords Deep tunnel · Tunnel roof collapse · Progressive failure · Functional catastrophe theory · Nonlinear power-law failure criterion · Dilatancy angle · Detaching velocity

List of symbols

Latin symbols

L_1 Half-width of the first collapsing block
 h_1 Intercept in y axis of the first collapsing block
 L_2 Half-width of the second collapsing block
 h_2 Intercept in y axis of the second collapsing block

R Tunnel radius
 w Thickness of the plastic detaching zone
 $g(x)$ Function describing the shape of a circular tunnel
 $f(x)$ Shape curves of the collapsing blocks
 $f_1(x)$ Shape curves of the first collapsing blocks
 $f_2(x)$ Shape curves of the second collapsing blocks
 m Nonlinear coefficient
 c_0 Initial cohesion of soil at zero stress
 J Functional of $f(x)$, total potential energy of the studied system
 U_i Strain energy of the internal forces on the detaching zone
 W_e Applied loads of the detaching surface
 P Parameter describing the variable detaching velocity
 Q Parameter describing the variable detaching velocity
 P_i Overall weight of each collapsing block

Greek symbols

ρ Weight per unit volume of the rock mass
 σ_n Normal stress on the failure surface
 τ_n Shear stress on the failure surface
 σ_t Absolute value of tensile stress when $\tau = 0$

✉ Kaihang Han
hankaihang@szu.edu.cn

Jiann-Wen Woody Ju
juj@ucla.edu

Heng Kong
hengkh@163.com

Mengshu Wang
wms32730@263.net

¹ Underground Polis Academy of Shenzhen University, Shenzhen 518060, China

² Department of Civil and Environmental Engineering, University of California, Los Angeles, CA 90095, USA

³ Beijing Municipal Construction Co., Ltd, Beijing 100048, China

⁴ School of Civil Engineering, Beijing Jiaotong University, Beijing 100044, China

ψ	Dilatancy angle
η	Dilatative coefficient
K_ψ	Dilatancy factor
γ^p	Plastic shear strain
η'	Angle between u and the vertical direction

1 Introduction

The stability of excavated tunnels remains one of the most important and difficult problems in geotechnical engineering. To reveal the collapse mechanism of tunnel roof is of high significance for providing reference for the design and construction of tunnels. However, geotechnical materials are filled with cracks and fractures, which make geotechnical materials random variability of mechanical properties and far more complex than traditional elastic–plastic materials. Researchers have developed a variety of analytical approaches to investigate the tunnel roof stability and reveal the collapse mechanism of tunnel roof. Analytical approaches mainly include the limit analysis methods (e.g., Atkinson and Potts 1977; Davis et al. 1980; Yang and Yang 2010; Wang et al. 2014; Sloan and Assadi 1993; Lyamin and Sloan 2000; Osman et al. 2006; Klar et al. 2007; Fraldi and Guarracino 2009, 2010, 2011, 2012; Yang and Huang 2011; Yang and Yao 2017; Huang and Yang 2011) and the catastrophe theory (e.g., Zhang et al. 2014a, 2016; Zhang and Han 2015; Yang et al. 2017).

Most of analytical approaches mentioned above mainly focused on the first collapse mechanism of tunnel roof; however, the phenomena of progressive failures are also very common and important in geotechnical engineering (e.g., Stone and Wood 1992; Santichaianant 2002; Costa et al. 2009; Jacobsz 2016; Zhang et al. 2014b). For example, some typical failure mechanisms including the development of failure patterns in active trapdoor model tests are shown in Fig. 1 (e.g., Stone and Wood 1992; Santichaianant 2002; Costa et al. 2009; Jacobsz 2016). With the vertical movement of the trapdoor, first failure surface initiates from the corners of the trapdoor and propagates toward the center of the trapdoor. Then, continued vertical movement of the trapdoor would lead to the developments of a series of new failure surfaces. In the final stage involving relatively large trapdoor movements, the failure surface is almost vertical. Figure 2 shows the progressive failure in roof collapse of deep and shallow tunnels in model tests (Zhang et al. 2014b). The plane strain model tests were conducted to investigate the failure modes and dynamic evolutionary rules of soft ground tunnels in urban areas under two different cover depths ($2.0D$ or $3.5D$ and D is tunnel diameter). As shown in Fig. 2a, b, the tunnel roof collapses under two different cover depths which are both progressive failure processes. Several collapses occur and at the same time several

short-term stable collapsing arches form during each collapse. The failure under the condition of $3.5D$ does not reach the ground surface while the failure under the condition of $2.0D$ affects the ground surface. Although many researches were conducted using the numerical simulations and the model tests, there are few analytical researches on the progressive failure of tunnel roof after the initial collapse for the complexity of this phenomenon.

Based on the above results of model tests, there are some features in progressive failure. First, the parameters characterizing the geotechnical materials are constantly changing and geotechnical materials undergo stress redistribution during the whole failure process. Second, failure surface propagation switches from one discontinuity to the next in a relatively sudden manner, which means that each collapsing block can be regarded as rigid. In this part, soil remains elastic and the total soil mass have displacement. Finally, soil dilatancy angle ψ defined as the vertical and the tangent along surface decreases from its initial value to zero and successive failure surfaces are in accordance with several discrete values of dilatancy angle ψ during the development of the successive failure surfaces (Stone and Wood 1992; Santichaianant 2002). In general, the phenomenon of progressive failure can be described as the continuous changes of system characteristic variables leading to several catastrophe changes of system state, which is fitting with the conception of the nature of the catastrophe theory (Thom 1972; Zeeman 1976; Arnold and Afraimovich 1999; Du 1994). Therefore, the catastrophe theory is well suited to analyze this kind of phenomenon.

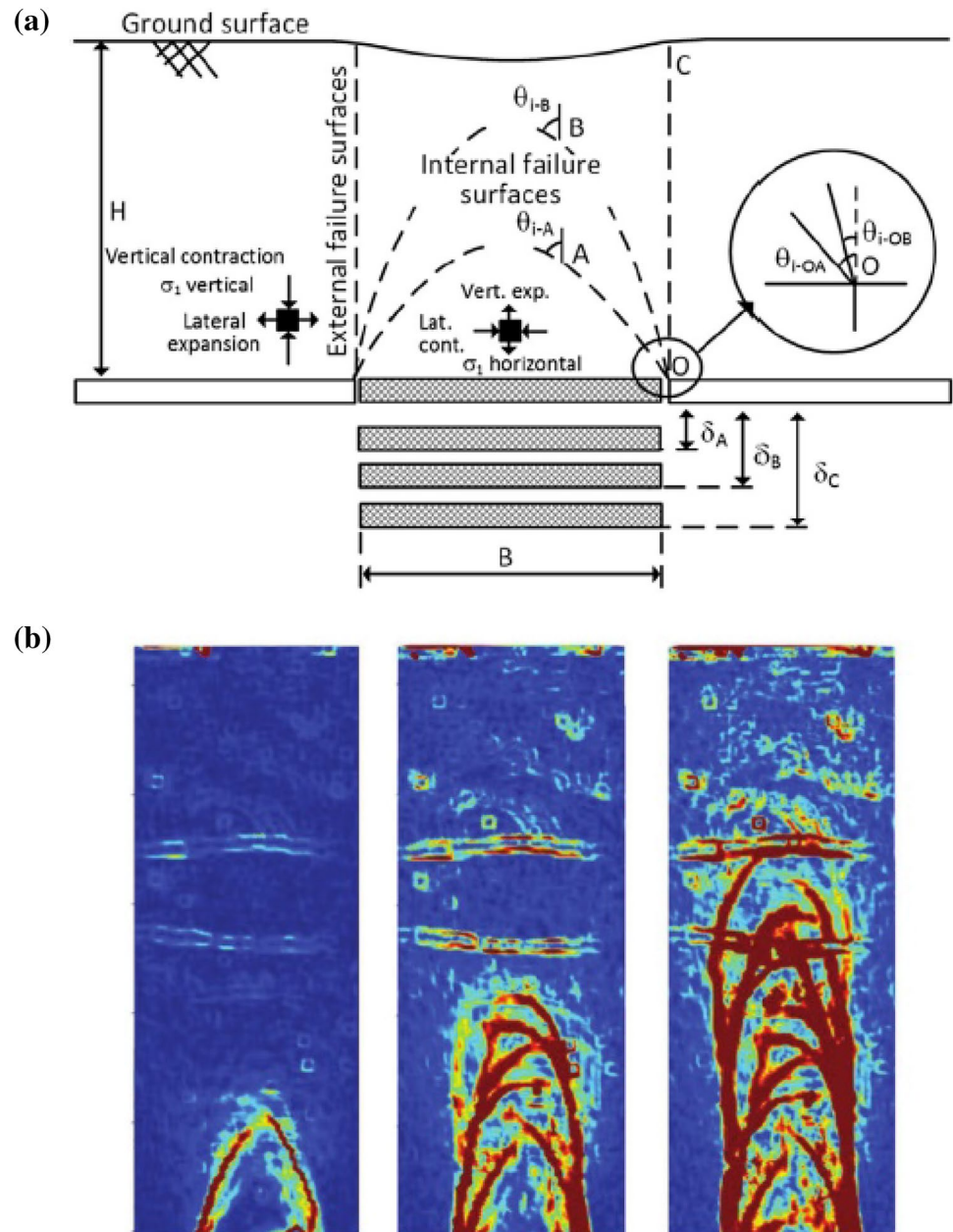
Using the functional catastrophe theory, the first failure collapse mechanisms was studied and the first possible shapes of the collapsing blocks for deep and shallow tunnels was derived, respectively (Zhang et al. 2014a; Zhang and Han 2015). In this paper, functional catastrophe theory is also used to investigate the progressive collapse mechanisms and collapsing block shapes of circular tunnels under conditions of plane strain. The analytical solutions for the shape curve of the collapsing block of deep circular tunnels are derived based on the nonlinear power-law failure criterion and the non-associated flow rule. Moreover, criteria on progressive failure occurrence for deep tunnels are derived. Then, the analytical predictions obtained in this paper are compared with the corresponding experimental testing results.

2 Problem Description

2.1 Progressive Failure Mechanism of the Tunnel Roof

The estimation of the roof stability of deep tunnels primarily lies in determining the shape and dimension of the

Fig. 1 Progressive failure in active trapdoor model tests (e.g., Stone and Wood 1992; Santichaianant 2002; Costa et al. 2009; Jacobsz 2016)



collapsing blocks which can actually collapse from the roof of the tunnel. To solve the proposed problem using the catastrophe theory, some assumptions are made. In this study, only the gravity field is considered, regardless of the tectonic stress field. The behavior of the rock mass is elastic-perfectly plastic. For the rock mass that follows the Hoek–Brown failure criterion, plastic potential energy within the total external load potential energy on the detaching surface is important and more dominant than elastic potential energy. Therefore, the paper ignores elastic potential energy and mainly concentrates on the plastic potential energy of the total external load potential energy on the detaching surface. The changes in the geometry of the collapsing block can

be regarded as insignificant through the onset of the collapse (rigid-plastic behavior), which is consistent with the results of experimental tests (e.g., Stone and Wood 1992; Santichaianant 2002; Costa et al. 2009; Jacobsz 2016; Zhang et al. 2014b). The problem is considered as under conditions of plane strain. Progressive failure in roof collapse of deep tunnel model tests shown in Fig. 2 is emphatically analyzed in this paper. Therefore, progressive failure mechanisms of a tunnel roof adopted in this paper is shown in Fig. 3, in which L_1 and h_1 are the half-width and the intercept in y axis of the first collapsing block and L_2 and h_2 are the half-width and the intercept in y axis of the second collapsing block, respectively. R is the tunnel radius, ρ is the weight per unit

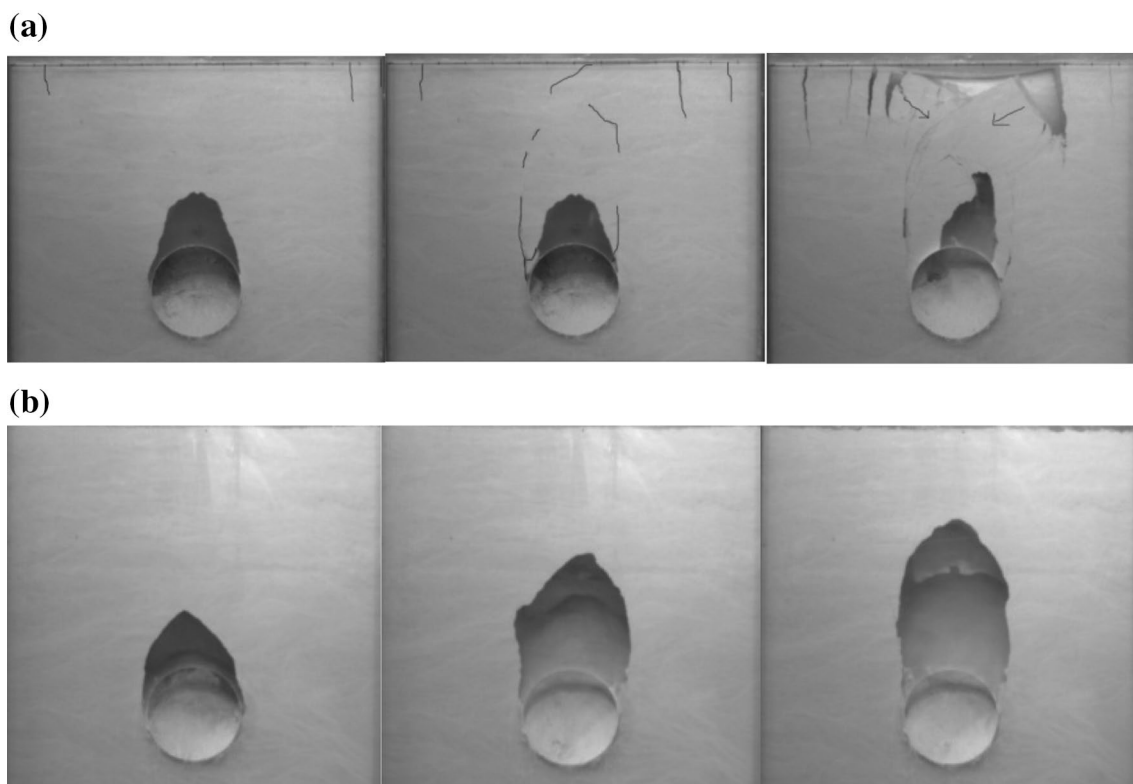


Fig. 2 Progressive failure of tunnel roof collapse in model tests: **a** progressive failure of surrounding rock under the condition of 2D depth; **b** progressive failure of surrounding rock under the condition of 3.5D depth (Zhang et al. 2014b)

volume of the rock mass, w is the thickness of the plastic detaching zone, and $g(x)$ is a known function describing the shape of a circular tunnel:

$$g(x) = -\sqrt{R^2 - x^2}. \tag{1}$$

The first consideration adopted in this paper is that the following derivation is based on the nonlinear failure criterion and the non-associated flow rule. Many experiments have shown that the failure envelop of soils is not linear in the σ_n - τ_n stress space, and the linear failure criterion is merely a particular case. Thus, a nonlinear failure criterion may be more suitable for the stability analysis of geotechnical structures. For this reason, the nonlinear power-law failure criterion is adopted in this paper, which can be expressed as follows (Zhang and Chen 1987; Zhang and Wang 2015; Yang and Yao 2017):

$$\tau_n = c_0 \left(\frac{\sigma_n + \sigma_t}{\sigma_t} \right)^{1/m}, \tag{2}$$

where c_0 = initial cohesion of soil at zero stress; σ_n and τ_n = normal and shear stresses on the failure surface, respectively; σ_t = absolute value of tensile stress when τ is equal to zero; and m = nonlinear coefficient.

Using the non-associated flow rule, the real deformation and failure characteristics of soil can be better simulated. Similar to the associated flow rule, the velocity at velocity discontinuities for a soil following a non-associated flow rule inclines at an angle, dilatancy angle ψ , with respect to the velocity discontinuity line. In general, the dilatancy angle ψ varies from zero to the friction angle φ ($0 \leq \psi \leq \varphi$). Correspondingly, dilative coefficient, η , which relates the dilatancy angle and the soil friction angle, is defined as:

$$\eta = \frac{\psi}{\varphi}. \tag{3}$$

Theoretically, the magnitude of dilative coefficient is $0 \leq \eta \leq 1$. The case $\eta = 1$ indicates that the material follows an associated flow rule. According to reference (Zhang and Wang 2015), when the geotechnical materials subject to nonlinear power-law failure criterion and non-associated flow rule, Eq. (2) can be modified to Eq. (4). For the sake of derivation, the term ηc_0 is replaced by a new parameter c_{0i} :

$$\tau_{ni} = \eta_i c_0 \left(\frac{\sigma_{ni} + \sigma_t}{\sigma_t} \right)^{1/m} = c_{0i} \left(\frac{\sigma_{ni} + \sigma_t}{\sigma_t} \right)^{1/m}. \tag{4}$$

The second key consideration adopted in this paper is that dilatancy angle ψ decreases from its initial value to zero and

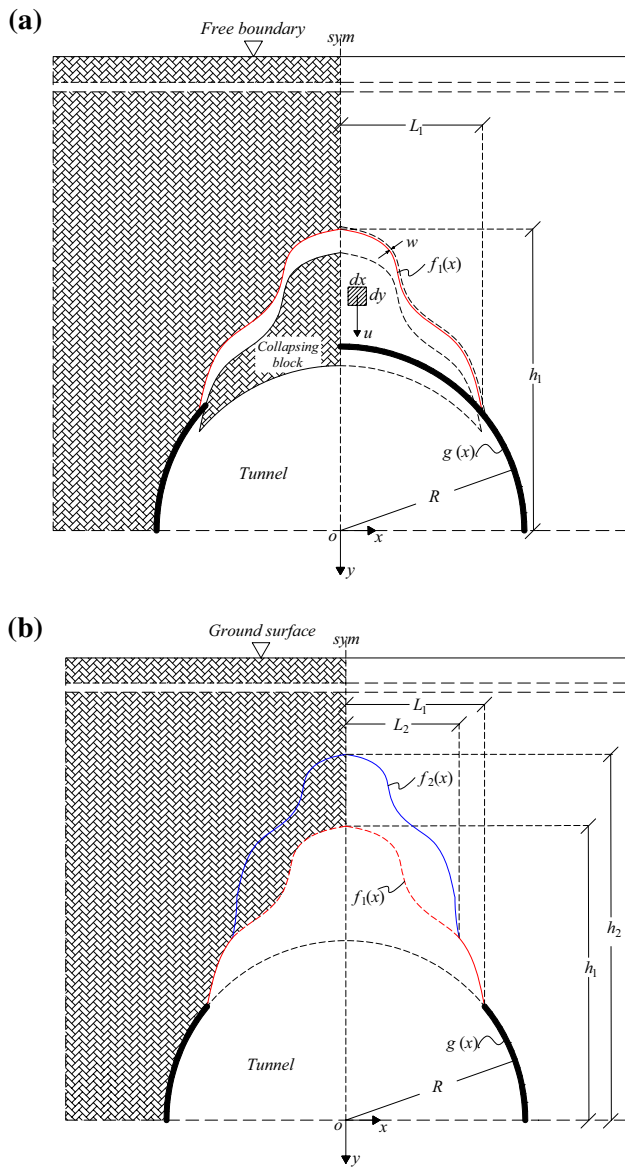


Fig. 3 Progressive failure mechanisms of the deep tunnel roof: **a** first collapsing block of a tunnel roof; **b** possible successive collapsing block of a tunnel roof

successive failure surfaces are in accordance with several discrete values of dilatancy angle ψ during the development of the successive failure surfaces. In addition, it should be pointed that the dilatancy angle ψ can be considered as a function of plastic strain and confining stress, and subsequently a dilatancy factor K_ψ that decays from an initial value K_ψ in accordance with an exponential function of plastic shear strain is proposed as follows (Detournay 1986; Alejano and Alonso 2005):

$$K_\psi = 1 + (K_{\psi,peak} - 1)e^{-\gamma^p / \gamma^{p*}}, \tag{5}$$

where $K_\psi = (1 + \sin\psi)/(1 - \sin\psi)$.

By making simple derivation, the variation of dilatancy angle ψ along with of plastic shear strain γ^p is as follows:

$$\sin \psi = \frac{\sin \psi_0}{\sin \psi_0 + (1 - \sin \psi_0)e^{\gamma^p / \gamma^{p*}}} \quad (\psi \text{ from } \psi_0 \text{ to } 0). \tag{6}$$

As shown in Eq. (6), dynamic (continuous) variation of plastic shear strain γ^p leads to dynamic (continuous) variation of dilatancy angle ψ , which results in dynamic (continuous) variation of dilative coefficient η in Eq. (4). However, based on the features in progressive failure mentioned above in Introduction, not the whole continuous values of dilatancy angle ψ correspond to the tunnel roof collapses but only several discrete values of dilatancy angle ($\psi_1, \psi_2, \psi_3, \dots$) correspond to several collapses. Therefore, the catastrophe state analysis of progressive failure lies in the derivation of the occurrence conditions for each collapse and determining the shape and dimension of the collapsing blocks.

The failure mechanism of tunnel roof (Fraldi and Guaracino 2009) is modified by considering variable detaching velocity along yield surface (Li and Yang 2017). And they concluded that the impact of variable detaching velocity is more remarkable on the shape of collapsing block. Therefore, the third key consideration adopted in this paper is the variable detaching velocity along detaching surface to obtain more consistent prediction results with the corresponding experimental testing results.

2.2 Catastrophe Theory and Catastrophic Conditions for a Functional

Since the deformation and failure of tunnel surrounding rock are characterized by nonlinear and discontinuous phenomena, catastrophe theory is suitable for investigating the behaviors of tunnel collapse. The nature of the catastrophe theory is continuous change of system characteristic quantity which leads to catastrophe change of system state. The results of model test show that several continuous collapses of tunnel roof correspond to several discrete value of dilatancy angle. Moreover, the dilatancy angle changes continuously with plastic shear strain. In other words, progressive failure can be considered as successive catastrophe phenomena, which means that continuous change of plastic shear strain γ^p leads to several catastrophe changes of system state.

If the potential function of the system is defined by a functional $J[f(x)]$, as in Eq. (7), determining the non-Morse critical point $f_c(x)$ of the potential function of the system becomes challenging:

$$J[f(x)] = \int_a^b F[x, f(x), f'(x)]dx, \tag{7}$$

where the primes indicate the derivatives of the functions with respect to their subscript coordinates, i.e., $f'(x) = \partial f(x)/\partial x$.

With a subsection integral, the two specific forms of the catastrophic conditions are obtained for functional $J[y]$ as follows (Zhang et al. 2014a; Zhang and Han 2015):

$$\frac{\partial F}{\partial f(x)} - \frac{\partial}{\partial x} \left(\frac{\partial F}{\partial f'(x)} \right) = 0, \quad (\text{Euler equation}), \quad (8)$$

$$\frac{\partial^2 F}{\partial f(x)^2} - 2 \frac{\partial}{\partial x} \left(\frac{\partial^2 F}{\partial f(x) \partial f'(x)} \right) + \frac{\partial^2}{\partial x^2} \left(\frac{\partial^2 F}{\partial f'(x)^2} \right) = 0, \quad (9)$$

(Catastrophic Euler equation).

3 Catastrophe State Analysis of a Deep Tunnel Collapse

3.1 First Collapsing Block of a Tunnel Roof

This paper proposed a new approach to determine critical state of tunnel roof collapse based on plastic strain energy and catastrophe theory. Based on the basic theory of elastic–plastic mechanics, the stress state of a point flows along the yield surface when the stress state of a point yields and the plastic strain energy of a point will increase. Therefore, the plastic strain energy can be used as an index to evaluate the state of the studied system. The larger the plastic strain is and the larger the accumulated plastic strain energy is. The collapse occurs when plastic strain energy reaches a certain value (i.e., critical state or catastrophic state).

To analyze the catastrophe state of a deep tunnel collapse, the total potential energy of the studied system should be first obtained. The total potential energy of the studied system includes the plastic strain energy of the internal forces on the detaching zone and the external force power induced by the weight of the detaching zone.

First, for standard geotechnical materials (i.e., those obeying to an associated flow rule), the plastic potential, Ψ , is assumed to be coincident with the nonlinear power-law yield curve and takes the following form by virtue of Eq. (4):

$$\Psi = \tau_{n1} - c_{01} \left(\frac{\sigma_{n1} + \sigma_t}{\sigma_t} \right)^{1/m}. \quad (10)$$

So that the plastic strain rate can be derived as follows:

$$\dot{\epsilon}_n = \lambda \frac{\partial \Psi}{\partial \sigma} = -\lambda \frac{c_{01}}{m \sigma_t} \left(\frac{\sigma_{n1} + \sigma_t}{\sigma_t} \right)^{(1-m)/m}, \quad (11)$$

$$\dot{\gamma}_n = \lambda \frac{\partial \Psi}{\partial \tau} = \lambda. \quad (12)$$

Moreover, from a purely geometrical line of reasoning, the plastic strain rate components can be written in the following form (Fraldi and Guarracino 2009):

$$\dot{\epsilon}_n = (\dot{u}/w) [1 + f'(x)^2]^{-1/2}, \quad (13)$$

$$\dot{\gamma}_n = -(\dot{u}/w) f'(x) [1 + f'(x)^2]^{-1/2}. \quad (14)$$

The comparison of Eqs. (13) and (14) shows that:

$$\lambda = -(\dot{u}/w) f'(x) [1 + f'(x)^2]^{-1/2}. \quad (15)$$

Then, substituting Eq. (15) into (11), it follows:

$$\dot{\epsilon}_n = (\dot{u}/w) f'(x) [1 + f'(x)^2]^{-1/2} \frac{c_{01}}{m \sigma_t} \left(\frac{\sigma_{n1} + \sigma_t}{\sigma_t} \right)^{(1-m)/m}. \quad (16)$$

Considering the compatibility, the plastic strain rate components in Eqs. (13) and (16) must be equated, that is:

$$\sigma_n = \sigma_t \left(\frac{m \sigma_t}{f'(x) c_{01}} \right)^{m/(1-m)} - \sigma_t. \quad (17)$$

Combining Eqs. (17) and (4), the following equation is obtained:

$$\tau_n = c_{01} \left(\frac{m \sigma_t}{f'(x) c_{01}} \right)^{1/(1-m)}. \quad (18)$$

Now the plastic strain energy of the internal forces on the detaching zone is derived using Eqs. (13) and (14), and (17) and (18):

$$U_i = \int (\sigma_n \epsilon_n + \tau_n \gamma_n) du = (u/w) [1 + f'(x)^2]^{-1/2} \left\{ -\sigma_t + \sigma_t^{1/(1-m)} \left(\frac{c_{01}}{m} \right)^{m/(m-1)} [1 - m] f'(x)^{m/(m-1)} \right\}. \quad (19)$$

For the geotechnical materials that obey non-associated flow rule, the plastic strain energy of the internal forces on the detaching zone should be modified into the following form (Li and Yang 2017) by virtue of two parameters P and Q :

$$U_i = \sigma_n \epsilon_n + \tau_n \gamma_n = Q \left[-\sigma_t + \sigma_t [c_{01}/(m \sigma_t)]^{m/(m-1)} (1 - m) \left[\frac{P}{Q} f'_1(x) \right]^{m/(m-1)} \right] \times u / \left[w \sqrt{1 + f'_1(x)^2} \right], \quad (20)$$

where P and Q are two parameters describing the impacts of variable detaching velocity on the shape curves of collapsing

blocks, which are defined as (η' is the angle between u and the vertical direction) (Li and Yang 2017):

$$\begin{cases} P = 1 + \frac{\tan \eta'}{f_1'(x)}, \\ Q = 1 - \tan \eta' f_1'(x). \end{cases}$$

In addition, the work of the applied loads per unit length (W_e) of the detaching surface is

$$W_e = \rho [f_1(x) - g(x)] u. \tag{21}$$

Then, the total potential energy of the studied system can be expressed as:

$$\begin{aligned} J[x, f_1(x), f_1'(x)] = & - \int_0^{L_1} \rho [f_1(x) - g(x)] u dx \\ & + \int_0^{L_1} Q \left[-\sigma_t + \sigma_t [c_{01}/(m\sigma_t)]^{m/(m-1)} (1 - m) \right. \\ & \left. \left[\frac{P}{Q} f_1'(x) \right]^{m/(m-1)} \right] u dx. \end{aligned} \tag{22}$$

Based on the functional catastrophe theory, the function F studied is

$$\begin{aligned} F = & F[x, f_1(x), f_1'(x)] \\ = & \left\{ -\rho [f_1(x) - g(x)] + Q \left[-\sigma_t + \sigma_t [c_{01}/(m\sigma_t)]^{m/(m-1)} (1 - m) \right. \right. \\ & \left. \left. \left[\frac{P}{Q} f_1'(x) \right]^{m/(m-1)} \right] \right\} u. \end{aligned} \tag{23}$$

The key in the catastrophic state analysis is to find the specific expression of $f_1(x)$ with the help of Eqs. (8) and (9).

Substituting Eq. (23) into Eqs. (8) and (9), the explicit forms of the group of differential equations of $f_1(x)$ for the problem are

$$-\rho - \frac{d}{dx} \left(-Q \left(\frac{P}{Q} \right)^{m/(m-1)} \sigma_t [c_{01}/(m\sigma_t)]^{m/(m-1)} m f_1'(x)^{1/(m-1)} \right) = 0, \tag{24}$$

$$\frac{d^2}{dx^2} \left(-Q \left(\frac{P}{Q} \right)^{m/(m-1)} \sigma_t [c_{01}/(m\sigma_t)]^{m/(m-1)} \frac{m}{m-1} f_1'(x)^{(2-m)/(m-1)} \right) = 0. \tag{25}$$

$$\begin{aligned} & \left\{ -\rho [f_1(L_1) - g(L_1)] + Q \left[-\sigma_t + \sigma_t [c_{01}/(m\sigma_t)]^{m/(m-1)} (1 - m) \left[\frac{P}{Q} f_1'(L_1) \right]^{m/(m-1)} \right] \right\} \\ & - [f_1'(L_1) - g'(L_1)] \left[-Q \left(\frac{P}{Q} \right)^{m/(m-1)} \sigma_t [c_{01}/(m\sigma_t)]^{m/(m-1)} m f_1'(L_1)^{1/(m-1)} \right] = 0. \end{aligned} \tag{32}$$

The detaching curve $f_1(x)$ is obtained by integrating Eq. (24):

$$f_1(x) = Q P^{-m} (\sigma_t \rho^{m-1} / c_{01}^m) (x + \rho^{-1} \tau_0)^m - h_1, \tag{26}$$

where τ_0 and h_1 are two integration constants.

Substituting Eq. (26) into (25), the following equation is obtained:

$$\frac{P^m}{Q} \left(\frac{\rho^{2-m} c_{01}^m}{\sigma_t} \right) \left(\frac{2-m}{m} \right) (x + \rho^{-1} \tau_0)^{-m} = 0. \tag{27}$$

Equation (27) is required to be zero for any value of x . This means that the value of m must be 2, which is the result of Eq. (9), i.e., one of the catastrophic conditions. In addition, the parameter m determines the power exponent of $f_1(x)$, so it also describes the shape of the collapsing block. Based on the value of m , the reduced form of $f_1(x)$ can be obtained:

$$f_1(x) = Q P^{-2} (\sigma_t \rho / c_{01}^2) (x + \rho^{-1} \tau_0)^2 - h_1. \tag{28}$$

There are two unknown parameters τ_0 and h_1 in Eq. (28), which can be determined by transversality conditions in variational analysis. It states that Eq. (23) should satisfy both Eqs. (29) and (30) (Zhang et al. 2014a; Zhang and Han 2015):

$$\left. \frac{\partial F}{\partial f_1'(x)} \right|_{x=0} = 0, \tag{29}$$

$$F - [f_1'(x) - g'(x)] \left. \frac{\partial F}{\partial f_1'(x)} \right|_{x=L_1} = 0. \tag{30}$$

Substituting Eq. (23) into Eqs. (29) and (30), the explicit forms of the transversality conditions are

$$\begin{aligned} & -\sigma_t [c_{01}/(m\sigma_t)]^{m/(m-1)} m f_1'(0)^{1/(m-1)} \\ & = -Q \left(\frac{P}{Q} \right)^{m/(m-1)} \sigma_t [c_{01}/(m\sigma_t)]^{m/(m-1)} \\ & \quad \times m \left[m (\sigma_t \rho^{m-1} / c_{01}^m) (0 + \rho^{-1} \tau_0)^{m-1} \right]^{1/(m-1)} = 0, \end{aligned} \tag{31}$$

Simplifying Eqs. (31) and (32), the values of τ_0 and h_1 in the expression of collapsing block are determined as follows:

$$\tau_0 = 0, \tag{33}$$

$$h_1 = Q(\sigma_i/\rho - g(L_1) + g'(L_1)L_1). \tag{34}$$

Substituting the values of τ_0 and h_1 into Eq. (28), the shape curve of collapsing block can be obtained as follows:

$$f_1(x) = Q \left\{ (\sigma_i \rho / c_{01}^2) \left(\frac{x}{P} \right)^2 - [\sigma_i / \rho - g(L_1) + g'(L_1)L_1] \right\}. \tag{35}$$

Now we obtain the curve which describes the shape and dimensions of the collapsing block of deep tunnels. The curve is a parabola with y axis being the axis of symmetry and h_1 being the y intercept.

However, the value of L_1 is still unknown in Eq. (35). Then the value of L_1 can be easily obtained using the geometric compatibility condition:

$$f_1(x = L_1) = g(x = L_1). \tag{36}$$

Substituting Eqs. (1) and (35) into Eq. (36) results in:

$$Q(\sigma_i \rho / c_{01}^2) \left(\frac{L_1}{P} \right)^2 - Q(\sigma_i / \rho) + (Q - 1)g(L_1) - Qg'(L_1)L_1 = 0. \tag{37}$$

From the mathematical perspective, whether or not the first collapse occurs is equivalent to whether Eq. (37) has a solution under the condition of $0 < L_1 < R$.

Moreover, it is possible to compute the overall weight of the first collapsing block per unit length (P_1) by

$$P_1 = 2 \int_0^{L_1} \rho [g(x) - f_1(x)] dx. \tag{38}$$

3.2 Possible Successive Collapsing Block of a Tunnel Roof

Similarly, the shape curves of possible successive collapsing blocks can be obtained as:

$$f_i(x) = Q \left\{ (\sigma_i \rho / c_{0i}^2) \left(\frac{x}{P} \right)^2 - [\sigma_i / \rho - f_{i-1}(L_i) + f'_{i-1}(L_i)L_i] \right\}. \tag{39}$$

Similarly, the value of L_i is still unknown in Eq. (39). Then the value of L can be easily obtained using the geometric compatibility condition:

$$f_i(x = L_i) = f_{i-1}(x = L_i). \tag{40}$$

Moreover, from the mathematical perspective, whether or not the successive collapse occurs is equivalent to whether Eq. (40) has a solution under the condition of $0 < L_i < L_{i-1}$.

Substituting Eqs. (35) and (39) into Eq. (40) results in:

$$L_i^2 = \frac{P^2}{\rho^2} \left(\frac{c_{0,i}^2 c_{0,i-1}^2}{c_{0,i-1}^2 - 2c_{0,i}^2} \right). \tag{41}$$

Considering the inequation $0 < L_i$, the result is as follows:

$$c_{0,i} < \frac{c_{0,i-1}}{\sqrt{2}} \text{ or } \eta_{i-1} < \frac{\sqrt{2}}{2}. \tag{42}$$

In addition, considering the inequation $L_i < L_{i-1}$, the result is as follows:

$$\eta_{i-1} < \frac{L_{i-1} \rho}{\sqrt{P^2 c_{0,i-1}^2 + 2L_{i-1}^2 \rho^2}}. \tag{43}$$

With Eqs. (42) and (43), the condition of progressive failure occurrence for deep tunnel based on nonlinear power-law failure criterion is as follows:

$$\eta_{i-1} < \min \left(\frac{\sqrt{2}}{2}, \frac{L_{i-1} \rho}{\sqrt{P^2 c_{0,i-1}^2 + 2L_{i-1}^2 \rho^2}} \right). \tag{44}$$

The occurrence of progressive failure in tunnel roofs from an analytical perspective was analyzed (Fraldi and Guarra-cino 2012) and it is demonstrated that within the framework of limit analysis after the collapse of a first block from the tunnel roof no additional detachments can take place (i.e., $\eta_{i-1} = 1$). This shows those results in Eq. (34) are consistent with the conclusion (Fraldi and Guarracino 2012). As a consequence, it is further confirmed that the attention must be focused mainly on degradation processes of the rock mass.

Moreover, it is possible to compute the overall weight of each collapsing block per unit length (P_i) by

$$P_i = 2 \int_0^{L_i} \rho [f_{i-1}(x) - f_i(x)] dx. \tag{45}$$

4 Comparisons with the Results of Model Test

The results obtained from this paper were compared with the results from model tests (Zhang et al. 2014b). The plane strain model tests were conducted to investigate the failure modes and dynamic evolutionary rules of soft ground tunnels in urban areas under different overburden depths. The geometrical similarity ratio of the model tests were 1/30. A kind of material, composed of barite, quartz and vaseline, was selected to represent the surrounding ground. The weight ratio of the ingredients barite:quartz:vaseline was

Fig. 4 Comparisons of analytical results with the results obtained from model test: **a** experimental testing results; **b** analytical results ($P=1, Q=1$)

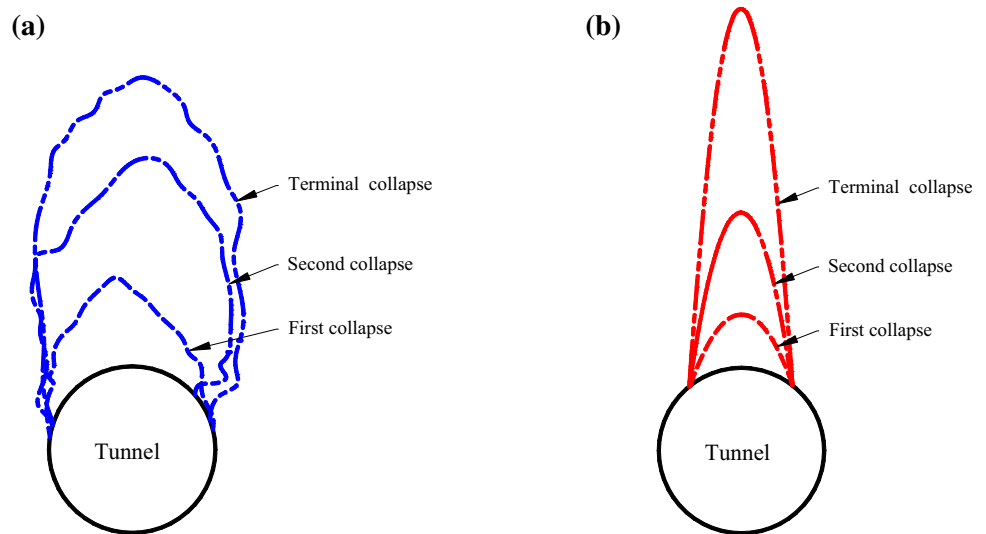


Table 1 Values of parameters in each collapse of model test

Parameters	First collapse	Second collapse	Final collapse
ψ_i	$\psi_1 = \varphi$	$\psi_2 = 0.64\varphi$	$\psi_3 = 0.44\varphi$
η_i	1	0.64	0.68
c_{0i} (kPa)	20	14.12	9.57
$f_i(x)$	$0.74x^2 - 4.95$	$1.80x^2 - 8.66$	$3.93x^2 - 16.09$

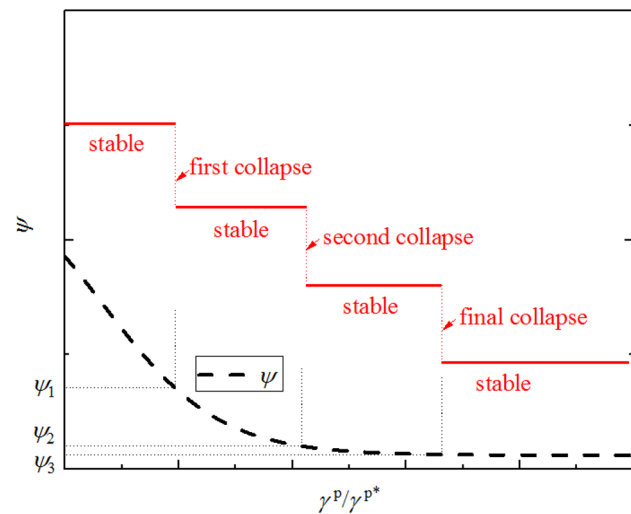


Fig. 5 Catastrophe state analysis of a deep tunnel collapse

8.0:5.0:0.6. The tunnel excavation process was modeled by the pressure release of an airbag inside the tunnel. The stress field of the model test was produced by gravity alone.

The comparison between the estimated values by experimental and analytical results is shown in Fig. 4. The specific initial values of parameters in this model test are $c_{01} = 20$ kPa, $\sigma_t = 22$ kPa and $\rho = 18$ kN/m³, $R = 3$ m. Table 1

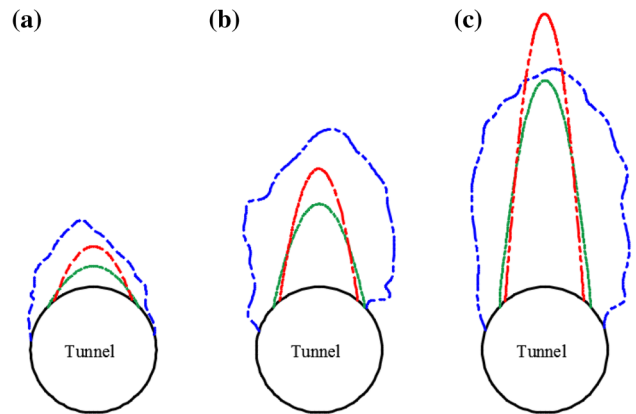


Fig. 6 Comparisons with two cases of P and Q : **a** first collapse; **b** second collapse; **c** final collapse (experimental testing results: blue curves; analytical results of $P=1$ and $Q=1$: red curves; analytical results of $P=1.2$ and $Q=0.8$: green curves) (color figure online)

shows the specific values of parameters in each collapse of model test.

The results show that the modes and rules of progressive failure of deep circular tunnel are similar. The authors claim that the precise extraction of dynamic test parameters is very difficult which leads to the differences of experimental and analytical results. Moreover, as shown in Fig. 5, only the variation of plastic shear strain γ^p (or dilatancy angle ψ) is considered and the variations of other parameters are not considered in this paper, which also leads to the differences of experimental and analytical results.

Furthermore, the impacts of variable detaching velocity on the shape curves of the several continuous collapsing blocks are shown in Fig. 6, which indicates that detaching velocity (P and Q) has a big effect on the shape curves of collapsing blocks. Therefore, variable detaching velocity

should be considered to obtain more consistent prediction results with the corresponding experimental testing results.

5 Conclusions

This paper uses functional catastrophe theory to investigate the progressive collapse mechanisms and collapsing block shapes of circular tunnels under conditions of plane strain. The main conclusions are as follows.

1. In general, the phenomenon of progressive failure can be described as the continuous changes of system characteristic variables leading to several catastrophe changes of system state, which is fitting with the conception of the nature of the catastrophe theory. Therefore, the catastrophe theory is well suited to analyze this kind of phenomenon and adopted in this paper.
2. The analytical solutions for the shape curve of the collapsing block of circular tunnels are derived based on the nonlinear power-law failure criterion and non-associated flow rule. Moreover, the conditions of progressive failure occurrence for deep tunnel were proposed. Those conditions would be used to judge whether or not the first and successive collapse occurs.
3. The analytical predictions obtained in this paper are compared with experimental testing results. The comparisons show that our analytical predictions are consistent with the corresponding experimental testing results, thus demonstrating the validity of the proposed analytical methodology.

Acknowledgements The authors appreciate the support from the Fundamental Research Funds for the Central Universities of China (Grant no. 2015YJS128).

References

- Alejano LR, Alonso E (2005) Considerations of the dilatancy angle in rocks and rock masses. *Int J Rock Mech Min Sci* 42(4):481–507
- Arnold VI, Afraimovich VS (1999) *Bifurcation theory and catastrophe theory*. Springer, Berlin
- Atkinson JH, Potts DM (1977) Stability of a shallow circular tunnel in cohesionless soil. *Géotechnique* 27(2):203–215
- Costa YD, Zornberg JG, Bueno BS, Costa CL (2009) Failure mechanisms in sand over a deep active trapdoor. *J Geotech Geoenviron Eng* 135(11):1741–1753
- Davis EH, Gunn MJ, Mair RJ, Seneviratne HN (1980) The stability of shallow tunnels and underground openings in cohesive material. *Géotechnique* 30(4):397–416
- Detournay E (1986) Elasto-plastic model of a deep tunnel for a rock with variable dilatancy. *Rock Mech Rock Eng* 19:99–108
- Du XF (1994) *Application of catastrophe theory in economic field*. Xi'an Electronic Science and Technology University Press, Chengdu (in Chinese)
- Fraldi M, Guarracino F (2009) Limit analysis of collapse mechanisms in cavities and tunnels according to the Hoek–Brown failure criterion. *Int J Rock Mech Min Sci* 46(4):665–673
- Fraldi M, Guarracino F (2010) Analytical solutions for collapse mechanisms in tunnels with arbitrary cross sections. *Int J Solids Struct* 47(2):216–223
- Fraldi M, Guarracino F (2011) Evaluation of impending collapse in circular tunnels by analytical and numerical approaches. *Tunn Undergr Space Technol* 26(4):507–516
- Fraldi M, Guarracino F (2012) Limit analysis of progressive tunnel failure of tunnels in Hoek–Brown rock masses. *Int J Rock Mech Min Sci* 50:170–173
- Huang F, Yang XL (2011) Upper bound limit analysis of collapse shape for circular tunnel subjected to pore pressure based on the Hoek–Brown failure criterion. *Tunn Undergr Space Technol* 26(5):614–618
- Jacobsz S (2016) Trapdoor experiments studying cavity propagation. In: *Proceedings of the 1st Southern African Geotechnical Conference*, Durban, South Africa, pp 159–165
- Klar A, Osman AS, Bolton M (2007) 2D and 3D upper bound solutions for tunnel excavation using ‘elastic’ flow fields. *Int J Numer Anal Methods Geomech* 31(12):1367–1374
- Li T, Yang X (2017) Limit analysis of failure mechanism of tunnel roof collapse considering variable detaching velocity along yield surface. *Int J Rock Mech Min Sci* 100:229–237
- Lyamin AV, Sloan SW (2000) Stability of a plane strain circular tunnel in a cohesive–frictional soil. In: *Proceedings of the Booker Memorial Symposium*, Sydney, NSW, Australia, pp 16–17
- Osman AS, Mair RJ, Bolton MD (2006) On the kinematics of 2D tunnel collapse in undrained clay. *Géotechnique* 56(9):585–595
- Santichaianant K (2002) *Centrifuge modeling and analysis of active trapdoor in sand*. Ph.D. Dissertation. University of Colorado
- Sloan SW, Assadi A (1993) Stability of shallow tunnels in soft ground. In: *Proceedings of the Wroth Memorial Symposium*, Thomas Telford, London, pp 644–663
- Stone KJL, Wood DM (1992) Effects of dilatancy and particle size observed in model tests on sand. *Soils Found* 32(4):43–57
- Thom R (1972) *Structural stability and morphogenesis*. Westview Press, Colorado
- Wang Z, Qiao C, Song C, Xu J (2014) Upper bound limit analysis of support pressures of shallow tunnels in layered jointed rock strata. *Tunn Undergr Space Technol* 43:171–183
- Yang XL, Huang F (2011) Collapse mechanism of shallow tunnel based on nonlinear Hoek–Brown failure criterion. *Tunn Undergr Space Technol* 26(6):686–691
- Yang F, Yang JS (2010) Stability of shallow tunnel using rigid blocks and finite-element upper bound solutions. *Int J Geomech* 10(6):242–247
- Yang XL, Yao C (2017) Axisymmetric failure mechanism of a deep cavity in layered soils subjected to pore pressure. *Int J Geomech* 17(8):04017031
- Yang X, Li Z, Liu Z, Xiao H (2017) Collapse analysis of tunnel floor in karst area based on Hoek–Brown rock media. *J Cent S Univ* 24(4):957–966
- Zeeman EC (1976) *Catastrophe theory*. Scientific American, New York
- Zhang XJ, Chen WF (1987) Stability analysis of slopes with general nonlinear failure criterion. *Int J Numer Anal Methods Geomech* 11(1):33–50
- Zhang C, Han K (2015) Collapsed shape of shallow unlined tunnels based on functional catastrophe theory. *Math Probl Eng* 2015(3):1–13
- Zhang J, Wang C (2015) Energy analysis of stability on shallow tunnels based on non-associated flow rule and non-linear failure criterion. *J Cent S Univ* 22(3):1070–1078

Zhang C, Han K, Fang Q, Zhang DL (2014a) Functional catastrophe analysis of collapse mechanisms for deep tunnels based on the Hoek–Brown failure criterion. *J Zhejiang Univ-Sci A* 15(9):723–731

Zhang C, Han K, Zhang D, Li H, Cai Y (2014b) Test study of collapse characteristics of tunnels in soft ground in urban areas. *Chin J Rock Mech Eng* 33(12):2433–2442 (in Chinese)

Zhang R, Xiao HB, Li WT (2016) Functional catastrophe analysis of collapse mechanism for shallow tunnels with considering settlement. *Math Probl Eng* 2016(11):1–11

Publisher's Note Springer Nature remains neutral with regard to jurisdictional claims in published maps and institutional affiliations.